INFLUENCE OF THE PARAMETERS PREHEATING TEMPERATURE AND LINEAR ENERGY ON THE MICROGRAPHIC AND MACROGRAPHIC CHARACTERISTICS OF WELDED JOINTS

Corneliu RONTESCU[1], Ionelia VOICULESCU[2], Gabriel IACOBESCU[3], Dumitru-Titi CICIC[4]

Lucrarea prezintă rezultatele experimentale obţinute în urma analizelor micro şi macrografice a îmbinărilor sudate obţinute prin sudarea rectilinie cu o sursă concentrată (TIG), pe componente din oţel slab aliat termorezistent.

Se analizează din punct de vedere micro şi macrografic cordoanele de sudură obţinute prin topiri superficiale fără material de adaos, în contextul păstrării constante a timpului de răcire $t_{8/5}$ concomitent cu variaţia celorlalţi parametri tehnologici ai regimului de sudare.

Din analiza imaginilor preluate ne rezultă faptul că structura şi granulaţia principalelor zone ale cordoanelor de sudură obţinute, în contextul păstrării constante a parametrului $t_{8/5}$, variază în funcţie de parametrii temperatură de preîncălzire-energie liniară aleşi.

The paper presents the experimental results obtained following the micrographic and macrographic analyses of the welded joints carried out by tungsten inert gas (TIG) welding with respect to components made of heat-resistant low alloy steel.

The beads obtained by superficial melting processes without filler material while keeping the cooling time $t_{8/5}$ constant and varying the other technological parameters of the welding process have been subject to micrographic and macrographic analyses.

Analyzing the processed images while keeping the $t_{8/5}$ parameter constant we found that the structure and granulation of the main zones of the obtained beads vary depending on the chosen parameters preheating temperature and linear energy.

Key words: $t_{8/5}$, TIG, welding, macrography, micrography

[1] Assist, Dept. of Material Technology and Welding, University POLITEHNICA of Bucharest, ROMANIA
[2] Prof., Dept. of Material Technology and Welding, University POLITEHNICA of Bucharest, ROMANIA, e-mail: gabiiacobescu@yahoo.com
[3] Prof., Dept. of Material Technology and Welding, University POLITEHNICA of Bucharest, ROMANIA
[4] Assist., Dept. of Material Technology and Welding, University POLITEHNICA of Bucharest, ROMANIA

1. Introduction

The characteristics of welded joints are directly influenced by the thermal processes that occur during the welding operations. At the same time the welding procedures influence the geometry of the joint, the nature and extent of the structural transformations, the level of the streses and deformations and the value of the resulted mechanical characteristics (hardness, resilience).

The local and concentrated action of the thermal sources on the welding material lead to the occurrence of complex, irregular and non-stationary thermal fields in the welding process [1].

The temperature distribution in the welded joints is influenced by the linear energy of the thermal source, by the thermophysical properties of the base material (specific heat, conduction of heat, material density and thermal diffusivity) and the heat loss to the environment [2].

The analytical observance, in accordance with the requirements of the industrial practice, of the thermal cycles during welding requires the consideration of three ways of heat propagation during welding and according to certain simplified physical models: three-dimensional propagation, two-dimensional propagation and intermediary propagation.

In order to analyze the characteristic of the thermal cycle during welding based on one indicator, the cooling time between the successive temperatures of 800^0C and 500^0C respectively, marked with $t_{8/5}$ is used at present. We noticed that the cooling time is in inverse ratui to the cooling speed, i.e. a higher $t_{8/5}$ value means a lower cooling speed and vice versa [3].

All the calculation relations for $t_{8/5}$, as well as its measuring zones by the thermographic method presented below refer exclusively to the quasi-stationary thermal fields. At the beginning and end of the layer (non-stationary field), the cooling speeds can also be twice as high as in the middle of a long layer.

2. Theoretical considerations

From the point of view of the metallurgic effects the cooling time $t_{8/5}$ is used for the characterization of the thermal cycle of a TIG welded joint. Its calculation is carried out differently, depending on the type of heat propagation.

For the welded joints we used samples made of low alloy heat-resistant steel (13CrMo4.4); the chemical composition of this material is presented in table 1, the specimenhad the dimensions 125 x 300 x 10 mm.

Table 1

Chemical composition of the low alloy heat resistant steel 13CrMo4.4

Element	C Max. [%]	Mn [%]	P max. [%]	S max. [%]	Si [%]	Mo [%]	Cr [%]
Content	0.15	0.48	0.0079	0.0058	0.25	0.43	1.1

Considering the thickness of the parts to be welded, the following calculation formula for the two-dimensional propagation was used for the calculation of the cooling time $t_{8/5}$:

$$t_{8/5} = (4300 - 4{,}3T_0) \cdot 10^3 \cdot \frac{Q^2}{d^2} \cdot \left[\frac{1}{(500 - T_0)^2} - \frac{1}{(800 - T_0)^2} \right] \cdot F_2 \quad (1)$$

where: $t_{8/5}$ = cooling time between 800^0C and 500^0C [s]

T_0 = initial temperature of the base material [^{0}C]

d = thickness of the sample to be welded [mm]

F_2 = shape factor that takes into account the deviations from the idealized physical model (for depositing a layer on a plate it is equal to 1) [4].

Q = linear energy [kJ/mm]

$$Q = \frac{U \cdot I}{v_s} \cdot \eta \cdot 10^{-3} \quad \text{[kJ/mm]} \quad (2)$$

U = voltage of the electric arc [V]

I = intensity of the welding current [A]

v_s = welding speed [cm/min.]

η = efficiency of the welding procedure (TIG welding, according to EN 1011-1/98 - η=0,6)

Considering the risk of cold cracking encountered at this class of low alloy heat resistant materials, the experimental procedure will take into consideration the limit values of the maximum hardness in the heat affected zone (HAZ) and of the minimum preheating temperature.

In order to reduce the risk of cold cracking for the resulted welded joints, the value of the maximum hardness in HAZ is set to 350 HV10 for this case. The critical value of the cooling time $t_{8/5}$ is calculated based on this value of the maximum hardness in HAZ – this value amounts to approximately 12s.

Three particular cases were taken into account for conducting the experimental program:

- case 1 – $t_{8/5}$=10s: in this case the welding technology is not observed and under these circumstances the obtained cooling time is under the limit cooling time;

- case 2 – $t_{8/5}$=15s: limit case, in this case the applied welding technology leads to a cooling time a little higher than the limit cooling time, in which case it is possible, due to the combined action of certain objective factors, to accidentally increase the hardness value, thus leading to the occurrence of the cracking risk;

- case 3 - $t_{8/5}$=20s: in this case the welding technology is observed and the risk of occurrence of the cracks in the presence of hydrogen is minimized.

Preheating and the maintenance of a certain temperature between the layers are necessary for the prevention of cold cracking in the base material, in the heat affected zone and/or weld deposit.

A minimum preheating temperature and maintaining the joint under a certain maximum temperature are necessary for obtaining the welds. If during the welding process the temperature increases very much, there is a risk of decrease in the corrosion strength of the material.

Bibliographic reference [3] points out that - from the point of view of the influences exercised by preheating temperature (T_{pr}) on the structure - the observance of this case takes place by taking into account the non-isothermal decomposition diagram of undercooled austenite (TTTC), overlapped by the cooling curves corresponding to the various values of the cooling time between 800^0…500^0C.

In order to determine the impacts of the application or non-application of the indicated welding technologies one established three research cases that simulate the limit conditions of the preheating temperature, as follows:

- case 1 – T_{pr}=30^{0}C: in this case, the welding technology is not observed, as the preheating temperature is not applied (T_{pr}=environment temperature);

- case 2 – T_{pr}=100^{0}C: in this case, the value of the recommended preheating temperature is not observed and the welding operation starts before the recommended preheating temperature is reached;

- case 3 – T_{pr}=200^{0}C: in this case, the temperature of the base material subject to the welding operation is higher than the recommended preheating temperature, but lower than the last temperature of the martensitic transformation.

For the calculation of the parameters of the welding process one took into account the recommendations of the manufacturer of refractory electrodes used during the experiments, WT20, diameter of 2.4 mm, while the welding arc voltage was U_a=15V.

In order to make the research easier and to conduct certain quantitative and qualitative comparisons of the results obtained during the experiments, one chose for the welding speed two values of 10, respectively 14 cm/min as per the recommended welding processes TIG [5].

Based on the values of the linear energy and taking into account the values of the arc voltage and of the previously chosen welding speed, after applying the calculation formula (2) one obtain the values of the welding current intensity that are necessary for the conduction of the experimental phase.

The values of the welding processes' parameters used during the experiments are presented in table 2.

Table 2

Parameters of the welding process

No. sample	$t_{8/5}$ [s]	T_{pr} [^{0}C]	E_l [KJ/cm]	I [A]	U [V]	v_s [cm/min]
1	10	30	9.19	170	15	10
2				238	15	14
3		100	7.84	145	15	10
4				203	15	14
5		200	5.91	109	15	10
6				153	15	14
7	15	30	11.25	208	15	10
8				292	15	14
9		100	9.59	178	15	10
10				249	15	14
11		200	7.23	134	15	10
12				187	15	14
13	20	30	12.99	241	15	10
14				337	15	14
15		100	11.08	205	15	10
16				287	15	14
17		200	8.35	155	15	10
18				216	15	14

3. Experimental procedure

During the experiments, the welding source is considered mobile and located in the middle of the plates. The thermal field is observed in the middle area of the joint so that the measurements are not influenced by the phenomena occurring in the beginning and end areas of the bead.

The welding operation was carried out under direct current, with direct polarity by using a TIG welding source with dropping external characteristic.

For the welded joints we used the set-up presented in figure 1:

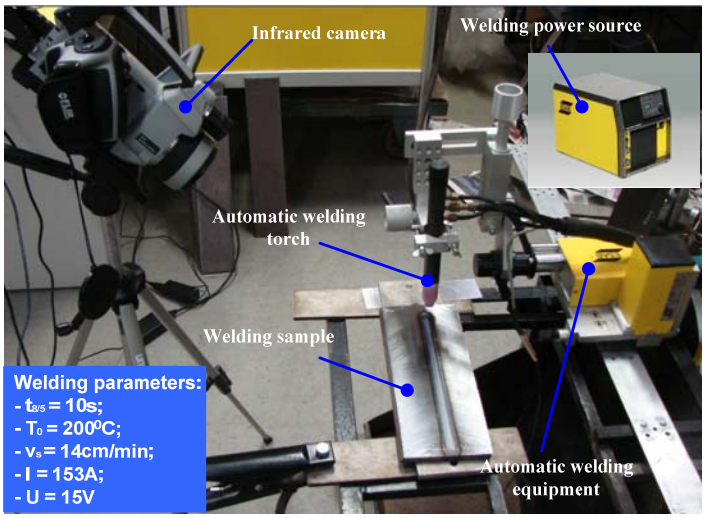

Fig. 1- Experimental set-up for automated WIG welding

In order to improve the parameters of the analyzed deposition processes one carried out a macroscopic and microscopic analysis. The samples were subjected to the attack with proper reagents, according to the type of analysis.

4. Results

The results obtained following the macrographic analysis, taken over with the help of the optical microscope EUROMEX are presented in fig. 2. By introducing them into specialized image-processing software one measured the characteristic dimension, penetration (p), width(B) and HAZ, as presented in table 3.

Another important parameter that can be determined after the end of the welding process and cooling of the joint, based on which one can determine the improved parameters of the welding technology, is the shape factor ψ as defined by the relation:

$$\psi = \frac{B}{p} \quad [-] \tag{3}$$

The values presented in table 3 were measured on the median direction in a cross-section on the longitudinal axis of the bead.

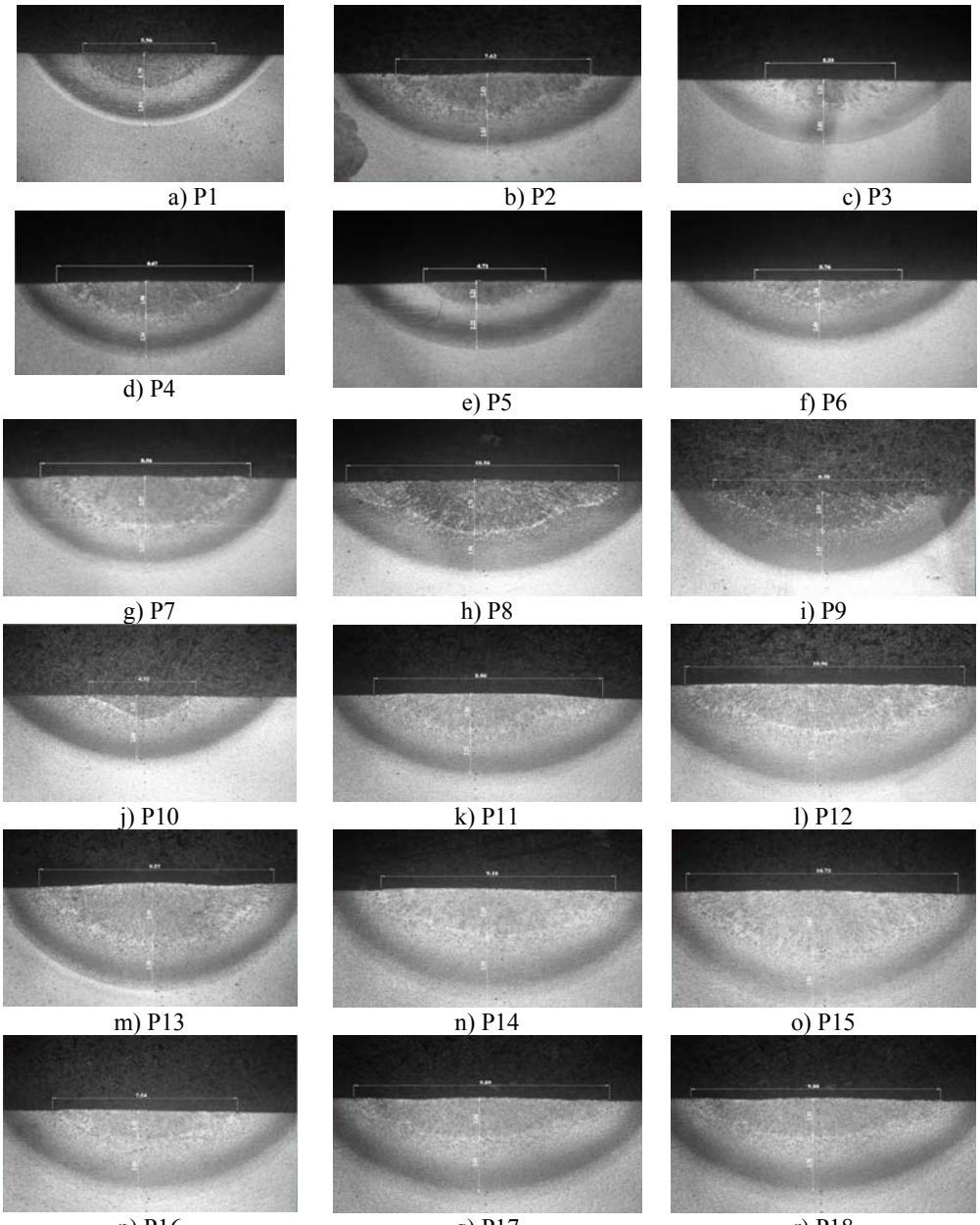

a) P1 b) P2 c) P3
d) P4 e) P5 f) P6
g) P7 h) P8 i) P9
j) P10 k) P11 l) P12
m) P13 n) P14 o) P15
p) P16 q) P17 r) P18

Fig. 2 – Characteristic dimensions of the beads

Table 3

Characteristic dimensions of the beads

Code sample	HAZ [mm]	B [mm]	p [mm]	ψ
P1	1.94	5.96	1.75	3.41
P 2	2.03	7.62	2.03	3.75
P 3	2.02	5.33	1.21	4.40
P 4	2.34	8.67	1.9	4.56
P 5	2.22	4.71	1.21	3.89
P 6	2.09	5.76	1.34	4.3
P 7	2.25	8.56	2.57	3.33
P 8	1.9	10.56	2.7	3.91
P 9	2.15	8.38	2.01	4.17
P 10	2.04	4.32	1.22	3.60
P 11	2.21	8.86	1.86	4.76
P 12	2.76	10.96	2.37	4.62
P 13	2.3	9.57	3.16	3.03
P 14	3.19	9.1	2.29	3.97
P 15	2.81	10.73	3.01	3.56
P 16	3.09	7.54	1.39	5.42
P 17	2.89	9.89	2.04	4.85
P 18	2.78	9.8	1.92	5.10

Based on the values indicated in table 3 one traced the variations of the characteristic dimensions of the bead B, p and HAZ.

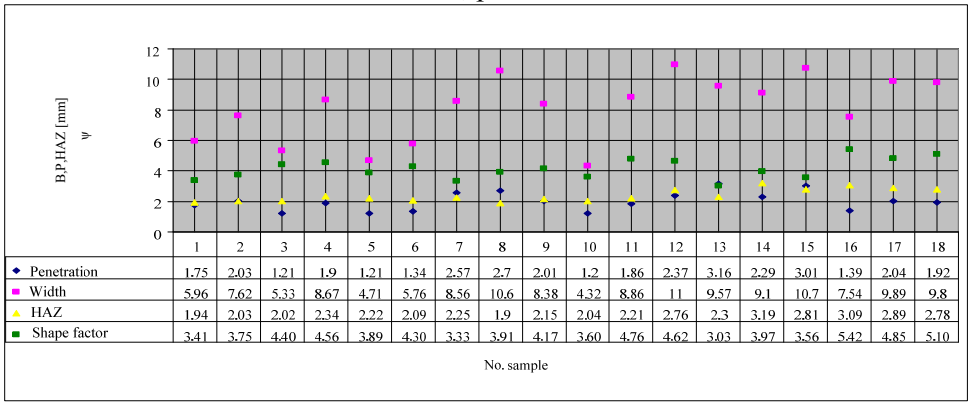

Fig. 3 – Graphic variation of the characteristic dimensions of the deposited beads

4.1. Extension of HAZ

If the cooling time $t_{8/5}$ amount is to 20 s, the distribution of the width values of the deposits related to these samples is much lower than in the other cases.

The analysis of the data presented in table 3, measured using an optical microscope, led to the following conclusions:

- for a value of $t_{8/5}$ of 10 s, the extension of HAZ is between 1.94 and 2.34 mm;
- for a value of $t_{8/5}$ of 15 s, the extension of HAZ is between 1.9 and 2.76 mm;
- for a value of $t_{8/5}$ of 20 s, the extension of HAZ is between 2.3 and 3.19 mm.

4.2. Joint width (B)

This characteristic was especially influenced by the value of the welding speed. The lowest values of the bead width were obtained for samples 5 – 4.71 mm (with E_l=5.91KJ/cm, v_s=10cm/min, T_{pr}=200^{0}C) and 10 – 4.32 mm (with E_l=9.59 KJ/cm, v_s=14 cm/min, T_{pr}=100^{0}C).

One observed that the T_{pr} effect on the bead width is prevalent, although the value of the linear energy for sample 5 is nearly half of the value of sample 10. In its turn, v_s that was lower for sample 5 determined the extension of HAZ in comparison to sample 10.

The maximum values of the width were obtained for samples 12 – 10.96 (with E_l=7,23 KJ/cm, v_s=14 cm/min, T_{pr}=200^{0}C) and 15 – 10,73 (with E_l=11,08 KJ/cm, v_s=10cm/min, T_{pr}=100^{0}C).

The values obtained in these cases are more than the double of the values presented above.

The effects of the increased linear energy were the extension of HAZ and the increased joint width.

4.3. Penetration value (p)

The lowest penetration values were obtained for samples 3 – 1.21 mm (with E_l=7.84 KJ/cm, v_s=10cm/min, T_{pr}=100^{0}C) and 5 – 1.21 mm (with E_l=5,91KJ/cm, v_s=10cm/min, T_{pr}=200^{0}C).

The maximum penetration values were obtained for samples 13 (with E_l=12.99 KJ/cm, v_s=10cm/min, T_{pr}=30^{0}C) and 15 (with E_l=11.08 KJ/cm, v_s=10cm/min, T_{pr}=100^{0}C).

For sample 15, the maximum values of the penetration and bead width were obtained under the maximum value of the considered cooling time.

For the same values of the parameter $t_{8/5}$=10 s, the variations of the dimension were of 0.4 mm for HAZ, 3.96 mm for the bead width, and 0.82 mm for the penetration.

For the same values of the $t_{8/5}$=10 s parameter, the variations of the dimension were of 0.86 mm for HAZ, 6.64 mm for the bead width and 1.5 mm for the penetration.

For the same values of the $t_{8/5}$=15 s parameter, the variations of the dimension were 0.89 mm for HAZ, 3.19 mm for the bead width and 1.77 mm for the penetration.

4.4 Grain size of the characteristic zones

As far as the size of the grains of the secondary structure is concerned, one observed that the minimum value of the grains (in the bead 9.81 μm, in HAZ 5.09 μm, in the normalization zone and 14.15 μm in the overheating zone) was obtained for sample 1 (with E_l=9.19 KJ/cm, v_s=10 cm/min, T_{pr}=30^0C). The maximum value of the grains resulted for sample 18 for the bead – 31.10 μm, 32.45 μm in the overheating zone of the HAZ and 22.58 μm in the normalization zone. The results obtained following the electronic micrographic analysis, taken over using of the electronic microscope SEM INSPECT S, are presented in table 4.

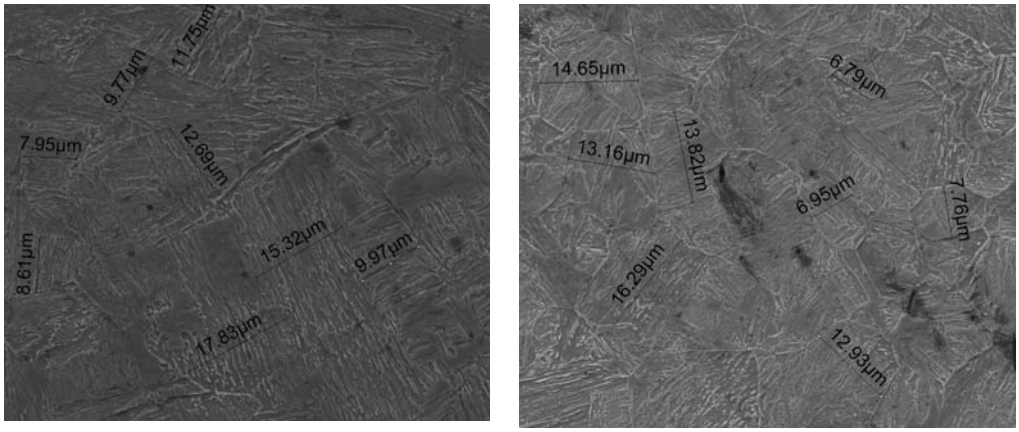

a) b)

Fig. 4 – General aspects concerning the size of the grain; a) bead; b) HAZ

Table 4

Size of the grains of the interest areas of the bead

Code sample	Bead [μm]	HAZ [μm]	
	Medium value	normalization	Overheating
P1	9.81	5.04	14.15
P 2	13.31	9.78	15.88
P 3	12.69	9.74	16.87
P 4	16.70	8.89	18.41
P 5	10.74	13.92	19.78
P 6	16.4	14.33	19.44
P 7	15.87	15.56	22.43
P 8	18.33	13.46	20.29
P 9	18.38	19.82	22.31
P 10	19.42	21.29	22.50
P 11	22.78	21.57	28.13
P 12	20.32	21.15	29.36
P 13	17.45	15.75	28.74
P 14	22.38	16.49	28.33
P 15	22.86	16.68	26.14
P 16	26.28	18.05	25.19
P 17	26.98	20.78	29.50
P 18	31.10	22.58	32.45

5. Conclusions

One discovered that the effect of the T_{pr} value on the extension of HAZ is predominant in relation with the increase in the value of the linear energy for welding (table 2; fig. 2 and fig. 3). This results from the measured values for the simulated preheating conditions and different values of the $t_{8/5}$ parameter.

The effects of the increase in the value of the linear energy during welding were the extension of the HAZ and the extension of the bead width.

Under similar thermal conditions ($t_{8/5}$ constant) the differences of the geometrical parameters of the welding bead are influenced by the variation of the values of the linear energy and of the preheating temperature.

For HAZ, the polyhedral grains go through less evident morphological transformations, while the increase is relatively uniform in relation to the initial geometric configuration.

By analyzing the evolution of the size of the grains in HAZ one drew the following conclusions:

- the granulation of the secondary structure resulted after the application of the welding process increases with the decrease in the cooling speed, that is with the increase in the value of $t_{8/5}$;

- the granulation of the structure increases with the increase in the maximum temperature that is reached in the interest zone during the thermal cycle

and with the increase in the duration during which the part is maintained above the overheating temperature;

- for a given case, the value of $t_{8/5}$ does not depend only on T_{pr} but also on the couple T_{pr}-linear energy;

- for obtaining the same value of $t_{8/5,}$ the value of T_{pr} is not equivalent with the value of the linear energy, due to the different way in which these parameters influence the overheating processes in HAZ.

B I B L I O G R A P H Y

[1]. *L. Miloş,* Procese de sudare, Editura Politehnica, Timisoara, 2006.
[2]. *E. Scutelnicu*, s.a. Modelarea proceselor termomecanice de asamblare, Editura Fundatiei Universitare Dunărea de Jos, Galati, 2003.
[3]. *V. Miclosi,* Tratamente termice conexe sudarii prin topire a otelurilor-Vol.I, Editura Sudura, Timişoara, 2003.
[4]. *Gh. Solomon,* Elemente de teoria proceselor de sudare, Editura Bren, Bucuresti, 2001.
[5]. *Zgură, Gh., G. Iacobescu C. Rontescu, D.T. Cicic,* Tehnologia sudării prin topire, Editura Politehnica Press , Bucureşti, 2007.
[6]. *V. Miclosi, ş.a.,* Materiale şi tratamente termice pentru structuri sudate, Ed UPB, Bucureşti, 1993.
[7]. *V. Micloşi,* Tratamente termice conexe sudării, Vol. I, Ed. Sudura, 2003.
[8]. *Gh. Solomon,* Elemente de teoria proceselor de sudare, Editura Bren, 2001.
[9]. *C. Rontescu,* Cercetări privind optimizarea sudării oţelurilor slab aliate termorezistente, Teză doctorat, 2008.
[10]. *G. Iacobescu, ş.a.* - Echipamente pentru sudare, vol. I, Ed.Printech, Bucureşti, 1999.